Demonstration of a Plasmo-Thermomechanical Radiation Detector with Si_3N_4 Waveguide Optical Readout Circuit

Qiancheng Zhao, Mohammad Wahiduzzaman Khan, Parinaz Sadri-Moshkenani, Regina Regan, Filippo Capolino, and Ozdal Boyraz

Department of Electrical Engineering and Computer Science, University of California, Irvine, California, 92697, USA
oboyraz@uci.edu

Abstract: A plasmo-thermomechanical radiation detector based on suspended nano-antennas with a Si_3N_4 waveguide optical readout circuit has been demonstrated. The responsivity and noise equivalent power of the detector are measured to be $3.954\times10^{-3}\mu m^2/\mu W$ and $3.01\mu W/\sqrt{Hz}$, respectively.

OCIS codes: (130.3060) Infrared; (040.1880) Detection; (220.4241) Nanostructure fabrication.

1. Introduction

Thermo-mechanical bolometers rely on the temperature-induced deformation upon exposure to radiation. Thus, pursuing efficient light concentration is a fundamental challenge to generate a temperature gradient in nanostructures with sub-wavelength dimensions. Fortunately, the challenge has been addressed by metasurfaces which enhance radiation absorption by plasmonic resonance [1]. Although plasmonically enhanced MEMS/NEMS has emerged as a promising research direction, the complex off-chip readout system remains a challenging task that needs to be addressed for practical applications. Therefore, it is highly desirable to have compact on-chip transduction and readout.

Recently we proposed a bimetallic plasmo-thermal mechanical infrared detector that utilizes Si_3N_4 waveguide for on-chip readout [2]. The infrared energy is absorbed and converted into heat with the help of plasmonic nanostructures, leading to thermo-mechanical deformation of the suspended fishbone wires, and thus changing the waveguide attenuation. The design geometry is scalable and can be adjusted for visible to IR wavelengths. For demonstration purposes, here we present a plasmo-thermomechanical detector sensitive to near-IR and visible wavelengths. The device characteristics are tested at the target wavelength of 660 nm. The device exhibits a responsivity of 3.954×10^{-3} $\mu m^2/\mu W$, indicating that $1\mu W/\mu m^2$ radiation intensity increment will result in an increment of 3.954×10^{-3} modulation index. The device has a noise equivalent power of 3.01 $\mu W/\sqrt{Hz}$ which is dominated by the vibration of the coupling fibers. The 3dB bandwidth of the detector is characterized to be 9.6 Hz, corresponding to a time constant of 16.6 ms.

2. Device Model and Fabrication

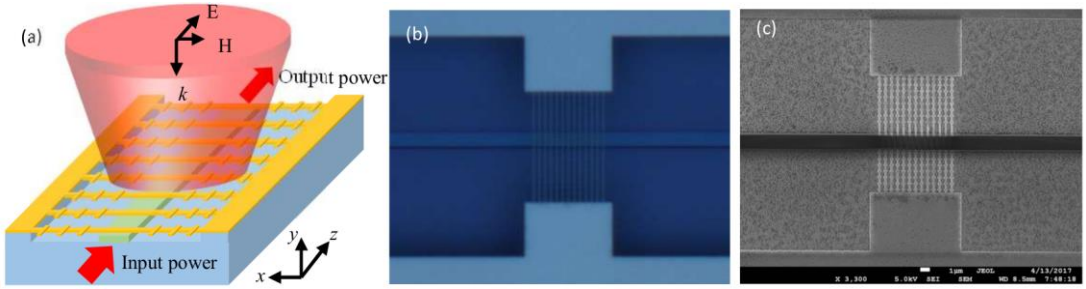

Figure 1 (a) The concept figure of the device. Top view of the (b) microscope image and (C) SEM image of the fabricated devices.

As demonstrated in Fig. 1(a), the plasmo-thermoplasmonic detector is composed of a Si_3N_4 waveguide and an array of bilayer fishbone nanowires that are suspended above the waveguide. When the electromagnetic radiation is transduced by the fishbone antennas to the nanowires, the temperature variation will thermally actuate the nanowires, and thus changes the gap between the nanowires and the waveguide top surface. The deformation of the nanowires can modulate the evanescent field from the waveguide, and hence alters the waveguide transmitted power. To build the devices, the Si_3N_4 waveguides, with a cross-section of 1.5 μm × 0.3 μm, are first fabricated and then coated by a SiO_2 sacrifice layer. Chemical mechanical polishing is used to planarize the sacrifice layer surface. The sacrifice layer thickness above the waveguide top surface, which is a critical parameter because it determines the gap between the nanowire and the waveguide, is monitored by hydrofluoric (HF) acid etching and stylus surface profiling, and thinned to be 62 nm by dry etching. Then the fishbone nanowire array is patterned and lithographed in an E-beam writer, followed by 3 nm Ti, 20 nm Ni and 30 nm Au metal deposition. The dimensions of the fabricated

structure stay close to our original design [3]. The sacrifice layer is finally removed by HF vapor etching to enable nanobridge suspension. The final device is depicted in Fig. 1(b) and (c).

3. Experimental Setup and Results

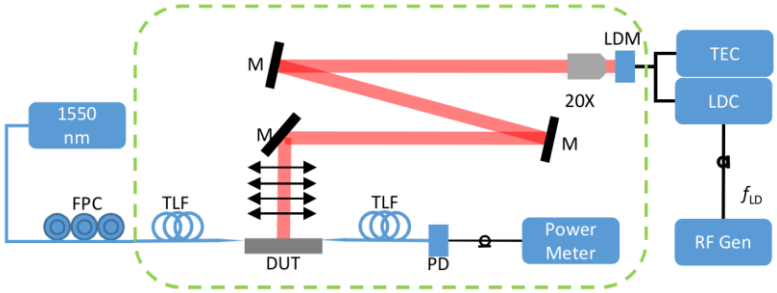

Fig. 2 Schematic of the experiment setup. 1550 nm: CW laser at 1550 nm wavelength; FPC: fiber polarization controller; TLF: tapered lensed fiber; DUT: device under test; PD: photodiode; M: mirror: 20X: objective lens with 20X magnification; LDM: laser diode mount; TEC: temperature controller; LDC: laser diode controller; RF Gen: radio frequency function generator. The dashed circle encloses the setups that are protected by air chamber.

Since the device has suspended structures, it is critical to avoid dust stuffing into the gaps between the nanowires and the waveguide top surface. Thus, an air flow chamber is used to protect the device and the main setups from dust. A continuous wave (CW) laser operating at 1550 nm wavelength serves as the source to provide the probe light. The probe light is coupled into the waveguide via a tapered lensed fiber (TLF). A fiber polarization controller (FPC) is inserted between the laser source and the TLF for polarization manipulation to maximize the coupling. The output light from the waveguide is collected by another TLF, and the collected power is measured by an optical power meter. The target light is provided by a 660 nm laser diode that is mounted in a laser diode mount (LDM) which is controlled by a temperature controller (TEC) and a laser diode controller (LDC). A function generator provides modulation to the LDC to vary the LD current. The generated laser is collected and collimated by an objective lens, and then redirected to the chip surface with the help of three mirrors. The radiation beam is normally incident to the device surface and its polarization (black arrows in Fig. 2) aligns with the antenna directions.

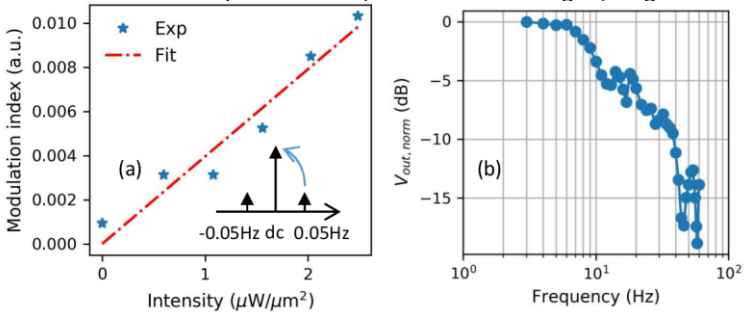

Fig. 3 (a) Modulation index as a function of the peak intensity. The inset shows the definition of the modulation index. (b) Normalized output voltage as a function of the modulation frequency.

The responsivity is defined as the ratio of the modulation index on the waveguide output power to the radiation intensity. The quasi-dc responsivity is quantified by the single tone measurement at 0.05 Hz modulation rate. By taking the Fourier transform of the temporal waveforms of the waveguide output power, the coefficient at the modulation frequency, 0.05 Hz, can be found. The modulation index is calculated by normalizing the coefficient at +0.05 Hz to its dc coefficient. As shown in Fig. 3(a), the modulation index is linearly curve-fitted with respect to the radiation intensity. The slope of the data (dotted-dashed line) shows the responsivity of the detector to be 3.954×10^{-3} μm^2/ μW. The noise equivalent power is 3.01 μW/$\sqrt{\text{Hz}}$. The noise mainly comes from the vibration of the tapered lensed fiber in waveguide coupling, and hence the results are system limited. The characterization of the frequency response is performed by sweeping the LDC modulation frequency and measuring the waveguide output power at synchronized frequencies via a lock-in amplifier. The voltage readout is normalized and plotted in Fig. 3(b). The 3dB cutoff frequency, f_{3dB}, is found to be 9.6 Hz corresponding to a time constant $\tau = 1/(2\pi f_{3dB}) = 16.6$ ms. The time constant, τ, is in the order of milliseconds like other thermal IR detectors [4]. It is worth mentioning that the device can be tailored for near- and mid-infrared detection by increasing the antenna dimensions [2]. A detailed study of optimized device geometry and thermodynamic response to increase the responsivity and bandwidth is being pursued.

This work was supported by the National Science Foundation under NSF Award # ECCS-1449397.

References

1. Y. Hui, et.al, "Plasmonic piezoelectric nanomechanical resonator for spectrally selective infrared sensing," Nat. Commun. **7**, (2016).
2. Q. Zhao, et.al, "On-Chip Bimetallic Plasmo-Thermomechanical Detectors for Mid-Infrared Radiation," IEEE Photonics Technol. Lett. (2017).
3. Q. Zhao, et.al, "Infrared Detection Using Plasmonically Enhanced Thermomechanically Actuated Nanowire Arrays," in CLEO. (2017).
4. F. Yi, et.al, "Plasmonically Enhanced Thermomechanical Detection of Infrared Radiation," Nano Lett. (2013).